A Study on Heat Transfer and Film Growth Rate During the III-V MOCVD Processes

임익태*, MASAKAZU SUGIYAMA**,
YOSHIAKI NAKANO**, YUKIHIRO SHIMOGAKI***

* 익산대학교 자동차과, ** Dept. of Electronic Eng., University of Tokyo,
*** Dept. ofMaterials Eng, University of Tokyo

Film growth of InP and GaAs using TMIn, TMGa, TBAs and TBP is numerically predicted and compared to the experimental results. To obtain exact thermal boundary conditions at the reactor walls, the gas flow and heat transfer are analyzed for full three-dimensional reactor including outer tube as well as the inner reactor parts. The results indicate that the exact thermal boundary conditions are important to get precise film growth rate prediction since film deposition is mainly controlled by the temperature dependent diffusion. The results also show that thermal diffusion plays an important role in the upstream region.

1. Introduction

Metalorgarnic chemical vapor deposition (MOCVD) is a widely used technology to grow thin epitaxial layers of various semi-conducting materials. Thin films of InGaAsP related materials grown by MOCVD process are widely used in optoelectronic devices such as laser diodes and optical modulators. To satisfy the needs of high quality films, it is very important to control film thickness and composition variations very precisely. Numerical simulations based on the computational fluid dynamics, CFD, have been used for decades successfully to design new or particular reactors or to find the optimized running conditions. The gas flow effects on the film growth were the dominant interests in the early stage of the reactor scale numerical modeling studies. The studies are expanded to model heat, mass transport and detailed chemical reaction models, thereafter [1]. Transport phenomena in a MOCVD reactor are very complex and to predict film growth rate accurately, gas flow, heat transfer, gas phase reactions and surface reactions are considered simultaneously. Therefore, CFD is a suitable way to predict the film growth rate during MOCVD processes.

In the recent communications [2], the authors' group reported a successful three-dimensional numerical modeling for the commercial horizontal MOCVD reactor using not only InP and GaAs but also tertiary and quaternary materials such as InGaAs and InGaAsP. In that research, however, the imposed boundary conditions for the reactor walls were obtained from the two-dimensional heat transfer analysis. The kinetic data for chemistry were adjusted

by the numerical experiments for the best fit with the experimental growth rate results.

In this study, the previous numerical model is expanded using a detailed three-dimensional thermal boundary conditions and experimentally measured kinetic data. To do this, film deposition mechanism is systematically studied at first, and then three -dimensional heat transfer calculation is carried to impose accurate thermal boundary conditions at the reactor walls. The effect of thermal diffusion is also considered which was not included in the previous study.

2. Numerical Model

The horizontal reactor (AIXTRON AIX200/4) shown in Fig. 1 was used for the simulations. The inner liner where the reactions occur is a rectangular conduit as shown at the top of Fig. 1 and surrounded by the cylindrical outer quartz tube. The inner liner is also made of quartz except of the central bottom portion where a graphite susceptor on which solid film is deposited is positioned. The inlet of the reactor is divided into two parts by a separator parallel to the graphite susceptor. Group III precursors such as trimethylgallium (TMGa) and trimethylindium (TMIn) are introduced to the upper inlet and group V precursors such as tertiary-butylarsine (TBAs) and tertiary-tutylphosphine (TBP) to the lower inlet close to the susceptor. The carrier gas is the hydrogen. Hydrogen gas is also used as a coolant between the inner reactor and the outer tube. Volumetric flow rate of the hydrogen cooling gas is 5 000 sccm. Actually two different grid systems were used to the simulations. The inner liner only was used for the growth rate simulations but the full reactor grid system was used to calculate the temperature calculations. Total mass flow rate in the inner reactor linear was 13 000 sccm and the operating pressure was 10 kPa. The precursors inlet partial pressures were 0.437, 0.573, 18 and 18 Pa for TMIn, TMGa, TBP and TBAs, respectively. The susceptor temperature was assumed to be uniform of 610(C. The commercial CFD software, FLUENT was used for the simulations.

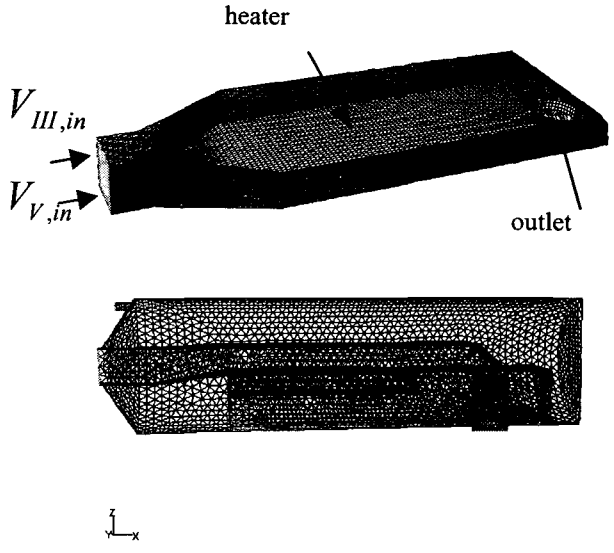

Fig. 1 Grid systems for the reactor including outer tube.

Governing equations for the transport phenomena in the reactor are continuity equation, momentum, energy and mass fractions conservation equations. Thermal diffusion is included in the mass fractions equations to find its effect. Gas mixture was considered as an ideal gas and the kinetic theory was used to calculate thermal conductivities or mass diffusivities of gas species. The required Lennard-Jones parameters shown in table 1 are the same as those of the previous study [3], which was obtained from the CHEMKIN thermodynamic database and the empirical relation given in the reference book [4].
Reaction chemistry used in this study is basically the same as our previous studies [2]. TMGa and TMIn were assumed to decompose to monomethylindium (MMIn) and monomethylgallium (MMGa), respectively, those were considered as intermediates to form solid film on the wafer surfaces. Intermediates for group V materials, TBAs and TBP were assumed to be AsH and PH. Pre-exponential factor, A and reaction energy, Ea, shown in table 2 was obtained from our group's experimental results [5]. Five times larger values of A than the original one for reaction II was used according to the mixing effect with group V gas. [6]

3. Results and Discussions

3.1 Film Growth Mechanisms

Fig. 2 and 3 show the predicted growth rate curves for InP and GaAs using temperature boundary conditions from the two-dimensional heat transfer analysis. Starting point is for the left hand edge of the graphite board. Symbols represent the experimentally measured results. Simulation results without considering thermal diffusion, dashed lines, show over prediction for the growth rate at the upstream region in both InP and GaAs cases. It can be said that thermal diffusion has to be included to the simulations.

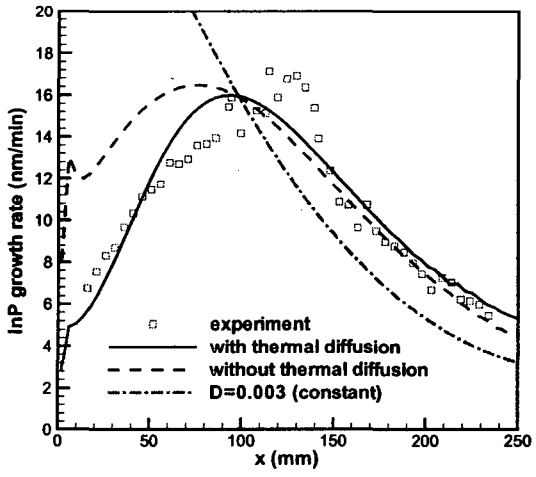

Fig. 2 Predicted growth rate curves with measured values for the InP film.

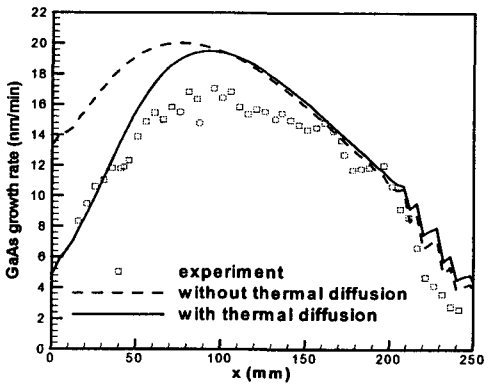

Fig. 3 Predicted growth rate curves with measured values for the GaAs film.

The slope of the growth rate curves at downstream part is controlled by mass diffusion according to our numerous simulation results. Detailed effects of mass diffusion on the

film deposition will be appeared in another report [7]. Simulations using constant value of the diffusivity failed to predict the deposition characteristics at the upstream region. In the upstream region, it seems impossible to obtain reasonable results using constant mass diffusivities. Therefore, we can say that temperature distribution is very important to get realistic simulation results because diffusion is largely affected by temperature distribution. Thermal diffusion effect is noticeable in the upstream region as shown in Fig. 2 and Fig. 3. Fig. 4 shows temperature distributions along the non-dimensionalized z-axis, perpendicular to the susceptor, at three points of x=0.12, 0.23, and 0.36, up, middle, and downstream of the reactor, respectively. We can see that temperature gradient at x=0.12 is very large compare to the other curves. This is the main reason of the thermal diffusion effect that is dominant at the upstream region shown in Fig. 2 and 3. In general, thermal diffusion is important in gas mixtures containing both heavy and light gas molecules [8]. Thermal diffusion causes large, heavy gas molecules to concentrate in cold regions, whereas small, light molecules concentrate in the hotter region of the reactor. In this study, thermal diffusion suppresses the growth rate mainly at the upstream region where the temperature gradient is large. When thermal diffusion is included, mass fractions of the gas species such as MMIn or PH are smaller than those of without including thermal diffusion, especially near to the surface.

Growth rate simulation results considering thermal effect show that the film growth is diffusion limited and thermal diffusion plays an important role. Therefore, to know exact temperature distribution is a necessary condition to obtain successful growth rate simulations. In the next section, we tried to calculate heat transfer using full three-dimensional model including radiation heat transfer.

3.2 Three-Dimensional Heat Transfer Calculation

In order to obtain precise temperature distribution of the reactor inner liner, three-dimensional heat transfer model for the whole reactor, including the outer tube, shown in Fig. 1 was developed. The graphite board, 3mm thickness and 267mm length, used to measure the reactor scale growth rate [2] was also included in the analysis. Heat conduction inside the quartz along the reactor walls was included. Working fluid was assumed to be hydrogen gas since partial pressures of the precursors were very small. Density of the gas was assumed to obey the ideal gas law. Materials properties such as specific heat, thermal conductivity and viscosity were calculated using fifth order polynomial function of temperature. Flow inside the reactor was treated as a laminar flow. Temperature of the heater surface was 883K according to the experimental condition.

Discrete transfer model was used to solve radiation heat transfer since hydrogen gas is considered as a transparent medium to infrared used for heating. Emissivity for quartz outer surface and graphite were set to be 0.8 and 0.65, respectively. Low emissivity for

quartz is due to the fact that film deposition on walls lowers emissivity and reactor wall temperature is dependent on the emissivity [9]. Heat transfer coefficient for the reactor outer tube walls was set to 7.5W/m-K that was given in the reference for the similar reactor [10]. Half of the reactor was used to the simulations because its shape is symmetrical. The number of total control volumes was 81 562.

Table 1 Lennard-Jones parameters used in the computation, ε/k is the potential well depths and σ is the collision diameters, respectively, where k is the

Species	ε/k (K)	σ (Å)
TMGa	378	5.52
MMGa	972	4.92
TMIn	454	5.62
MMIn	1049	5.02
TBAs	397	5.98
AsH	200	4.22
TBP	376	5.93
PH	190	4.07
C_4H_8	357	5.18
CH_4	141	3.75
H_2	38	2.92

Table 2 Reaction chemistry and reaction rate constants.

Gas-phase reactions			
$TMIn + H_2$	→	$MMIn + 2CH_4$	I
$TMGa + H_2$	→	$MMGa + 2CH_4$	II
TBAs	→	$AsH + C_4H_8 + H_2$	III
TBP	→	$PH + C_4H_8 + H_2$	IV
Surface reactions			
$MMIn + PH$	→	InP<s> + CH_4	V
MMGa +	→	GaAs<s> + CH_4	VI

Reactions	A (1/s)	Ea (kJ/mol)
I	1.86E15	186
II	1.2E15	196
III	5.32E15	203
IV	4.42E14	219
	A (m/s)	Ea (kJ/mol)
V	5E5	80
VI	1.23E9	130

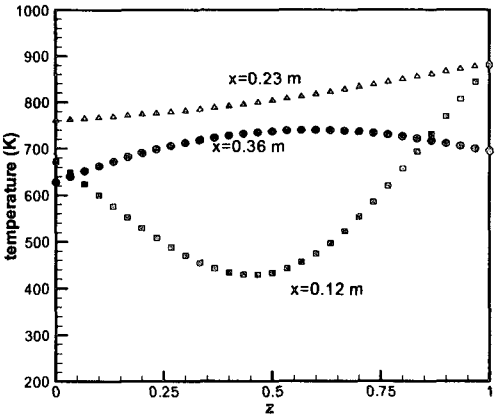

Fig. 4 Temperature profiles at upstream, middle and

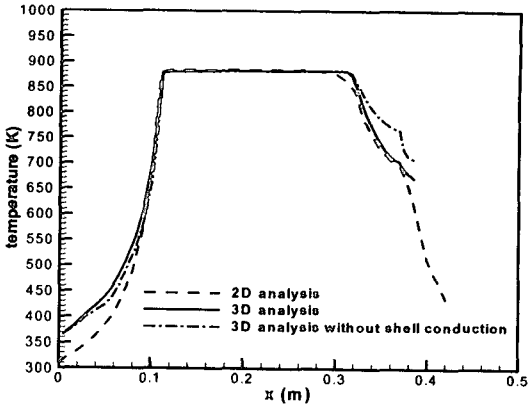

Fig. 5 Temperature profiles of the reactor inner liner bott dimensional calculations.om wall, conduction means axial conduction within the reactor quartz walls.

Fig. 5 and 6 show the temperature profiles obtained from two-dimensional and three-dimensional simulations. Fig. 5 is the bottom wall temperature profiles along the longitudinal direction of the inner reactor. The 3D analysis without shell conduction depicted by the dash-dot line means the results from without considering heat conduction along the thin walls of the reactor. Temperature from the three-dimensional calculation near the inlet is higher than that of the two-dimensional result represented by dashed line. It is thought to be due to the convective heat transfer effects because the axial conduction shows little influence and there is a circulation flow in three-dimensional results shown later.

As shown in Fig. 6, it is impossible to obtain the sidewall temperature distribution from two-dimensional simulation, so the same temperature profile as the upper wall was used to the growth rate simulations. But three-dimensional simulation results show that the sidewall temperature is much lower than the two-dimensional wall temperature. Fig. 7 shows the flow pathlines from the three-dimensional simulations. As previously mentioned,

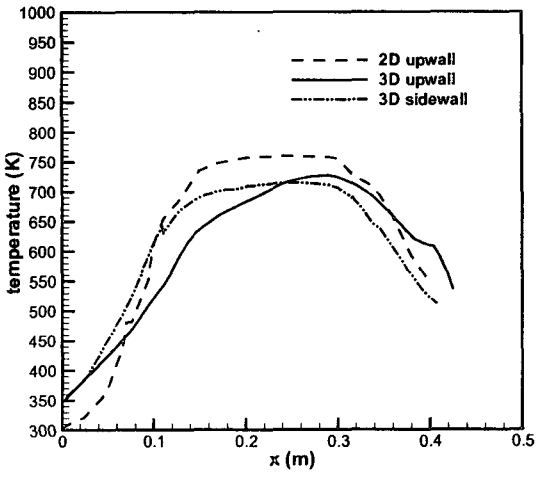

Fig. 6 Temperature profiles of the reactor inner liner up-wall and sidewall, axial conduction is included in 3-

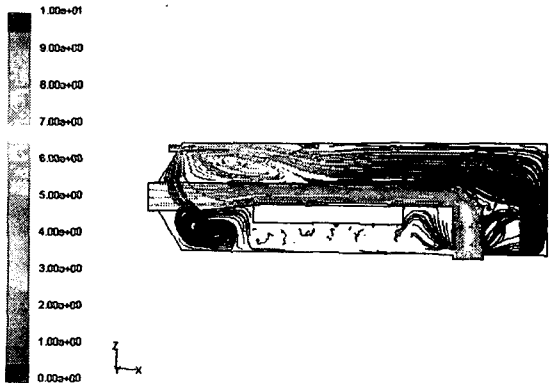

Fig. 7 Flow pathlines colored by velocity magnitude at the symmetry plane of the reactor from three - dimensional analysis.

gas is circulating at down of the inner liner in the upstream region but gas is nearly stagnant in two-dimensional analysis because cooling gas cannot flow between the outer tube and inner reactor conduit. This is maybe the main reason of the difference between two-dimensional and three-dimensional temperature profiles shown in Fig. 5.

Fig. 8 and Fig. 9 show the predicted growth rate curves for InP and GaAs using the thermal boundary conditions from two-dimensional and three-dimensional heat transfer analyses. The slope of the InP growth rate curve at the upstream region is in good agreement with the experiments in the case of using three-dimensional heat transfer boundary conditions. Effects of three-dimensional temperature analysis are more dominant in the GaAs case. The maximum point is largely lowered compared to the case of using two-dimensional temperature analysis. There are differences in the far downstream region compared to the experiments. This is thought to be that temperature is over-predicted at this region since constant heater temperature is used.

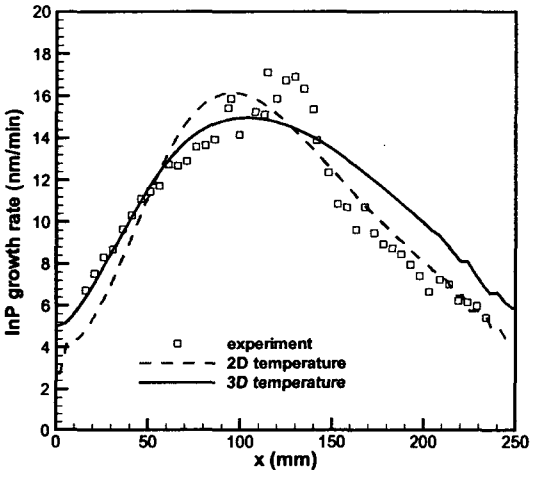

Fig. 8 Comparisons of the InP growth rate curves using two-dimensional and three-dimensional heat transfer analyses with experiments.

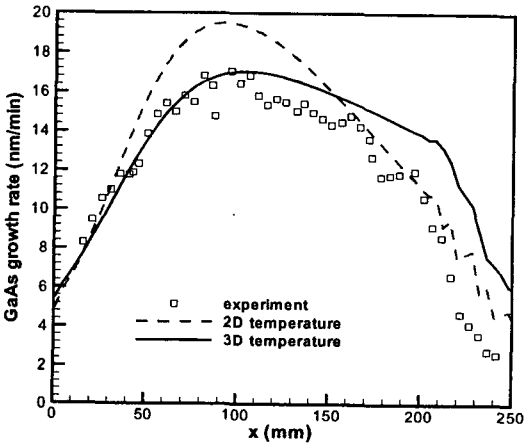

Fig. 9 Comparisons of the GaAs growth rate curves using two-dimensional and three-dimensional heat transfer analyses with experiments.

4. CONCLUSIONS

Temperature distribution of the reactor is calculated in two dimensions and three dimensions to find thermal effects on the film growth rate. Axial conduction through the reactor walls and radiation heat transfer were included to heat transfer analyses. Axial conduction has little influence except the outlet part of the wall. There is no great difference at the inner reactor up-wall temperature profile between two and three-dimensional analyses. But three-dimensional temperature profiles are different from the two-dimensional results at the bottom wall of the inner liner in upstream region and sidewall. It is shown that the exact temperature distribution is very important since the film deposition is mainly controlled by the temperature dependent diffusion. Film growth

rates of InP and GaAs are successfully predicted using three-dimensional temperature distributions without any parameter adjustment.

Acknowledgements

This work was supported by the Post-doctoral Fellowship Program of Korea Science and Engineering Foundation (KOSEF) through a grant of I.-T. Im and CREST of JST (Japan Science and Technology Agency).

References

[1] K. F. Jenson, 1989, J. of Crystal Growth, 98, pp. 148-166.

[2] O. Feron, M. Sugiyama., W. Asawamethapant, N. Futakuchi, Y. Feurprier, Y. Nakano, Y. Shmogaki, 2000, Appl. Surf. Sci.,159-160, pp. 318-327.

[3] O. Feron, M. Sugiyama, Y. Nakano, Y. Shimogaki, Electrochemical Soc. Pro. 2000, 13, pp. 707.

[4] R.C. Reid, J. M. Prausnitz, B. E. Poling, 1988, The Properties of Gases and Liquids, P. 586, McGraw-Hill, Singapore.

[5] H. J. Oh, M. Sugiyama, Y. Nakano, Y. Shimogaki, 2003, Jap. J. Appl. Phycs., Accepted.

[6] M. Sugiyama, K. Kusunoki, Y. Shimigaki, S. Sudo, Y. Nakano, H. Nagamoto, K. Sugawara, K. Tada, H, Komiyama, 1997, Appl. Surf. Sci., 117/118, pp. 746-752.

[7] I.-T. Im, H.J. Oh, M. Sugiyama, Y. Nakano, Y. Shimogaki, 2003, 11th Biennial (US) Workshop on OMVPE, OM22.

[8] C. R. Kleijn, 1995, Chemical Vapour Deposition Processes in Computational Modeling in Semiconductor Processing, Ed. by M. Meyyappan, p. 110-128.

[9] F. Durst, L. Kadinski Y. N. Makarov, M. Schafr, M. G. Vasil'ev, V.S. Yuferev, 1997, J. Crystal Growth, 172, pp. 389-395.

[10] R. Mucciato, N. Lovergine, 2000, J. of Crystal Growth, 221, pp. 758-764.